



## IMPACT STRENGTH OF GLASS AND GLASS CERAMIC

S. Bless and J. Tolman

Citation: [AIP Conference Proceedings](#) **1195**, 1421 (2009); doi: 10.1063/1.3295078

View online: <http://dx.doi.org/10.1063/1.3295078>

View Table of Contents:

<http://scitation.aip.org/content/aip/proceeding/aipcp/1195?ver=pdfcov>

Published by the [AIP Publishing](#)

---

### Articles you may be interested in

[Correlation between dielectric breakdown strength and interface polarization in barium strontium titanate glass ceramics](#)

*Appl. Phys. Lett.* **96**, 042902 (2010); 10.1063/1.3293456

[TEMPORAL SOFTENING AND ITS EFFECT UPON SPALL STRENGTH](#)

*AIP Conf. Proc.* **1195**, 965 (2009); 10.1063/1.3295306

[DETERMINING MATERIAL STRENGTH IN RAMP LOADING EXPERIMENTS](#)

*AIP Conf. Proc.* **1195**, 1023 (2009); 10.1063/1.3294973

[VARIATIONS IN THE SHEAR STRENGTH OF SHOCK LOADED NIOBIUM](#)

*AIP Conf. Proc.* **1195**, 1019 (2009); 10.1063/1.3294972

[Large-size ultrahigh strength Ni-based bulk metallic glassy matrix composites with enhanced ductility fabricated by spark plasma sintering](#)

*Appl. Phys. Lett.* **92**, 121907 (2008); 10.1063/1.2902282

---

# IMPACT STRENGTH OF GLASS AND GLASS CERAMIC

S. Bless and J. Tolman

*Institute for Advanced Technology, The University of Texas at Austin, Austin, TX 78759*

**Abstract.** Strength of glass and glass ceramic was measured with a bar impact technique. High-speed movies show regions of tensile and compressive failure. The borosilicate glass had a compressive strength of at least 2.2 GPa, and the glass ceramic at least 4 GPa. However, the BSG was much stronger in tension than GC. In ballistic tests, the BSG was the superior armor.

**Keywords:** Glass, PDV.

**PACS:** 62.20.F-, 62.20.mt, 06.40.-k.

## BAR IMPACT TESTS

The bar impact tests with photonic Doppler velocimeter (PDV) diagnostics are discussed in a companion paper given at this conference [1]. The PDV measures both the speed of the flyer plate before impact and the speed of the distal end of the bar after impact. It provides a measure of compressive and tensile strength, as discussed in [1], using the relationship

$$\sigma = 1/2uZ_b \quad (1)$$

where  $Z_b$  is the impedance of the bar, which may be approximated by the acoustic impedance,  $\rho c_b$ ,  $c_b$  being the bar wave speed given by the square root of Young's modulus divided by density. The impact drives a stress wave into the material whose amplitude is determined by

$$\sigma_i = Z_b Z_p v / (Z_b + Z_p) \quad (2)$$

where  $Z_p$  is the projectile impedance,  $\rho c_L$ . If the bar does not fail on impact, a wave of amplitude  $\sigma_i$  is generated. If the bar does fail, the wave amplitude is  $Y$ , the unconfined compressive strength.

## MATERIALS

The materials used in these studies were commercial borosilicate glass (BSG) and glass ceramic. BSG density is 2.2 g/cm<sup>3</sup>, and Young's modulus is 62 GPa,  $c_b = 5.31$  mm/ $\mu$ s. The glass ceramic (GC) is 25% nanocrystalline spinel; density = 2.78 g/cm<sup>3</sup>,  $E = 93$  GPa, and  $c_b = 5.78$  g/cm<sup>3</sup>. The BSG samples were 13 mm round by 152 mm long. The GC rods were 10 mm square by 102 mm long. Impactors were steel or tungsten rods that were larger than the target bar; these strikers were slightly indented by the impact.

## DATA

The shots conducted are listed in Table 1. For definition of maximum, minimum, and final free surface velocity, refer to Fig. 3 in [1], namely  $\sigma_m$  is the stress determined from the maximum velocity,  $\sigma_f$  from the final velocity, and  $\sigma_s$  from the spall signal [ $(Z_b(\max - \min \text{ velocity})/2)$ ]. In shots 29–31, the striker was changed from hard steel to tungsten in order to be sure that we drove the glass ceramic to an impact stress that was well above its strength. In shots 13, 14, and 15, retroreflective tape was attached to the bar. As discussed in [1], the maximum free surface velocity and spall signal may have been slightly clipped in these shots. A

graded impedance tape was attached to the impact surface in shots 11, 12, 14, and 15. As discussed in [1], use of the tapes seems to systematically lower the peak stress. Also, full data were only available in shots in which the PDV was used.

**TABLE 1.** Data

SN	proj	bar	V (m/s)	$\sigma_i$	$\sigma_m$	$\sigma_f$	$\sigma_s$
3	steel	BSG	266	2.4		1.44	
4	steel	GC	260	3.0		2.41	
7	steel	GC	250	2.9		1.78	
8	steel	BSG	250	2.3		1.30	
11	steel	GC	245	2.8	2.65	2.25	0.56
12	steel	BSG	264	2.4	1.73	1.35	0.89
13	steel	GC	280	3.2		1.28	
14	steel	GC	255	2.9	1.29	0.96	0.16
15	steel	BSG	255	2.3	1.22	0.91	
17	steel	BSG	310	2.8	2.16	1.79	1.09
27	steel	BSG	222	2.0	1.76	1.38	0.60
28	steel	BSG	225	2.0	1.73	1.58	0.74
29	WA	GC	455	6.1	4.01	3.05	0.06
30	WA	GC	516	6.9			
31	WA	GC	505	6.8	3.00	2.81	0.31

### HIGH-SPEED IMAGES

A Cooke eight-frame image converter camera was used to record the failure sequence in many of these experiments. Generally, eight frames are available from each shot. Frames at early, mid, and late times for each material are shown in Figs. 1–5. There is sometimes a faint ghost image of the later frames over the first frame image.

The basic sequence of events observed in the photographs is the same for both materials. A white-appearing disturbance propagates down the bar from the impact zone. The velocity of this disturbance is about equal to  $c_b$ ,  $(E/\rho)^{1/2}$ . We believe the white appearance is due to activation of surface flaws. There is a region of much more radial expansion near the face of the projectile, which stands off a few diameters and then advances with the projectile velocity. This region has clearly experienced compressive comminution.

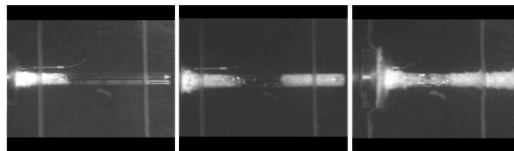


**Figure 1.** Photos from shot 5, BSG.

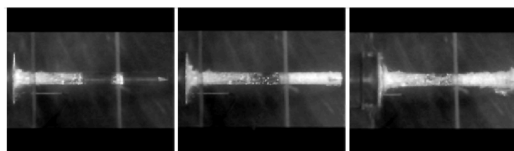


**Figure 2.** Photos from shot 8, BSG.

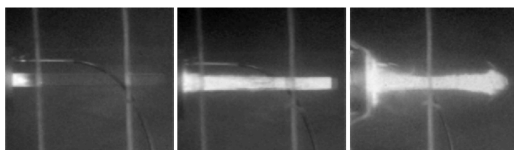


**Figure 3.** Photos from shot 4, GC.

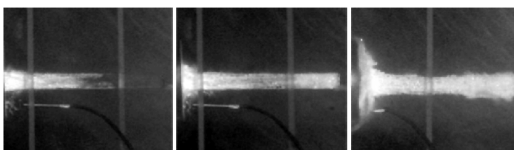


**Figure 4.** Photos from shot 7, GC.

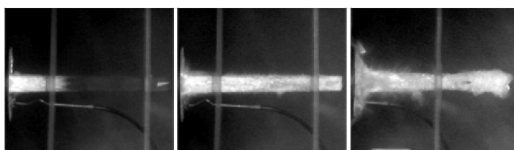


**Figure 5.** Photos from shot 11, GC.

There is a delay between impact and start of motion of the rear surface of the projectile that exactly agrees with the transit time for a longitudinal acoustic wave from impact at the distal end of the bar. Reflection of the wave from the rear surface soon produces a region in which tensile-failure/radial expansion occurs virtually simultaneously over several diameters, starting from the rear surface. In both of these materials, the rear expansion is slightly irregular, suggesting it originates from discrete flaws that cause asymmetry in the fracture pattern. In glass, there is a central section of the target bar that fails quite

late, or perhaps not at all. This behavior is less pronounced in the glass ceramic.

### STRESS AND STRENGTH IN BARS

Values of stress computed from final free surface velocity are shown in Fig. 6. These stress values are presumed to be a little less than the peak stress carried by the impact-generated wave; the larger the spall strength, the greater the difference. Data with the graded density impact are flagged with a circle as less reliable.

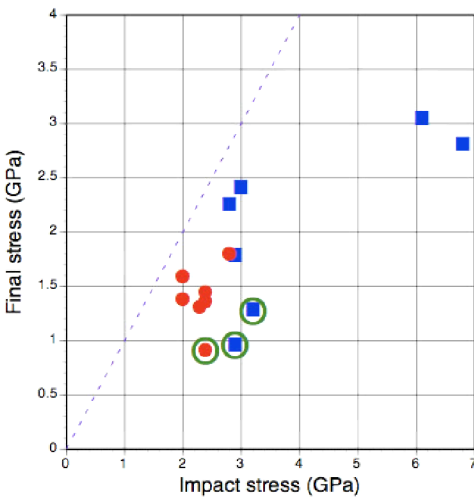


Figure 6. Strength measured from final velocity. BSG: circles. GC: squares.

Figure 7 shows the data for peak stress. While there are fewer data points, they more accurately reflect the peak stress in the bar.

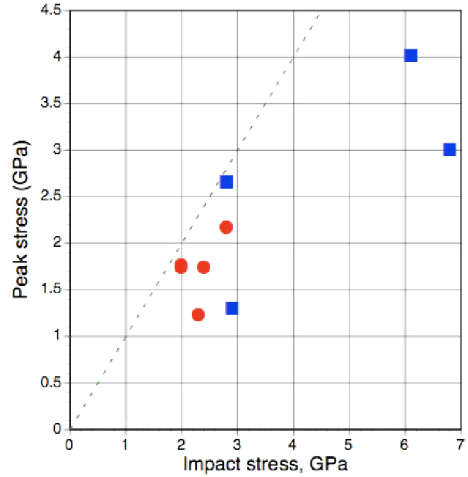
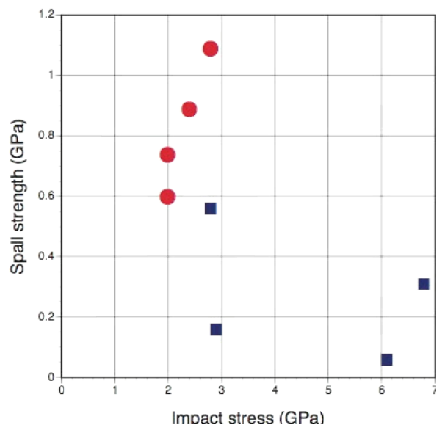


Figure 7. Peak stress in bars. BSG: circles. GC: squares.

In principle, peak stress values should follow the dotted line until  $\sigma_i > Y$ , after which the values should be constant and equal to  $Y$ . Clearly that is not the case. Evidently glass is very sensitive to premature failure at the impact face, which occurs before the peak stress rises to the intrinsic material strength. The best interpretation of the data is that the strength of the glass is the greatest stress amplitude that was able to propagate in the material. In this case, that value is 2.6 GPa for BSG, and 4 GPa for glass ceramic.

Figure 8 is the tensile strength data. The peak tensile stress in these bars is probably an extrinsic, as opposed to an intrinsic, property. Intact BSG glass, for example has a spall stress in excess of about 2.5 GPa. The failures seen here are presumably due to surface flaws. The peak tensile stress is a competition between the stress rate in the interior due to wave reflection, and relaxation due to a failure wave that travels inward from the surfaces.

The strength of the glass ceramic is much less than glass and decreases with pre-stress levels. This may well be an intrinsic stress. It is low because the heterogeneity in glass ceramic provides nucleation sites for tensile failure.



**Figure 8.** Peak tensile stress, as a function of impact stress. BSG: circles. GC: squares.

### BALLISTIC STRENGTH

A measure of the ballistic strength is provided by depth-of-penetration tests. A projectile is shot at a sample material of thickness  $T$  and penetration is measured into a substrate  $P_R$ . Such tests were conducted with BSG and GC, using a 6061T6 aluminum substrate, and bonding with double-sided window mounting tape, about 1 mm thick. The projectile was a .50 caliber fragment-simulating projectile (FSP)—an HRC30 13 g steel cylinder, with a half-flat nose. Impact velocities were 1100 to 1200 m/s. The results are shown in Fig. 9.

Surprisingly, the superior compressive strength of GC does not result in superior ballistic performance but to the contrary. It would appear that for this class of materials struck by this type of projectile, tensile strength is much more important than compressive strength.

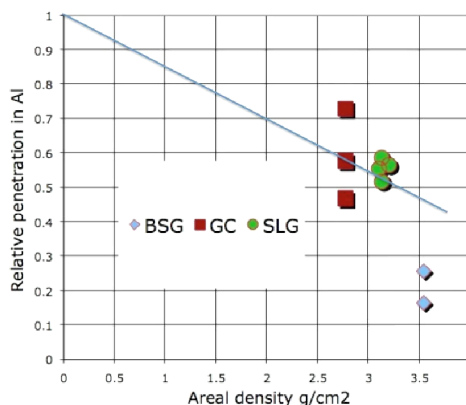


**Figure 9.** DOP data for various glasses and glass ceramic. Plotted is reduction of penetration in aluminum due to armor material vs. areal density of armor material.

### ACKNOWLEDGMENTS

The research reported in this document was performed in connection with award number N-00014-06-1-0475 from the Office of Naval Research. The views and conclusions contained in this document are those of the authors and should not be interpreted as presenting the official policies or position, either expressed or implied, of the US Government unless so designated by other authorized documents.

### REFERENCES

1. S. J. Bless, J. Tolman, S. Levinson, and J. Nguyen, "Improved Bar Impact Tests using a Photonic Doppler Velocimeter," 16th American Physical Society Topical Conference on Shock Compression of Condensed Matter, June 28–July 3, 2009, Nashville, TN.